Modeling Uranium-Proton Ion Exchange in Biosorption

JINBAI YANG AND BOHUMIL VOLESKY*

Department of Chemical Engineering, McGill University, 3610 University Street, Montreal, Quebec, Canada H3A 2B2

Biosorption of uranium metal ions by a nonliving protonated *Sargassum fluitans* seaweed biomass was used to remove the heavy metal uranium from the aqueous solution. Uranium biosorption isotherms were established for solution pH values ranging from pH 2.5–4.0. Uranium biosorption uptake was accompanied by the release of protons from the biomass. The sorption isotherms were highly pH dependent, and the metal binding increased significantly with increasing pH values. Above pH 3.0, the maximum uranium uptakes exceeded the total biomass binding capacity as expressed in equivalents units. A mathematical model based on the ion exchange between protons in the biomass and hydrolyzed uranium ion species was developed. Given the total uranium concentration and pH value, the model can calculate the uranium and proton binding as well as the composition of uranium ionic groups in the solution and on the biosorbent. The model was capable of fitting and predicting biosorption isotherms for different pH values as well as the equilibrium uranium desorption concentrations.

Introduction

Biosorption of dangerous elements from nuclear waste liquids has attracted a significant attention in recent years (*1*, *2*). Uranium is one of the most seriously threatening heavy metals because of its high toxicity and some radioactivity. Excessive amounts of uranium have found their ways into the environment through activities associated with the nuclear industry (*3*). Uranium contamination poses a threat in some surface and groundwater (*4*, *5*). Various nonliving biomass types such as those of filamentous fungi, yeast, bacteria, actinomycetes, etc., have been reported to bind uranium in excess of 150 mg/g of dry biomass (*6–10*). Freshwater algae such as *Chlorella regularis* and *vulgaris* also demonstrated a good uranium adsorption performance (*11*, *12*). The capability of marine algae to biologically concentrate radionuclides such as radium, thorium, and uranium has been known for a long time (*13*). Recently, uranium biosorption on a brown alga *Sargassum fluitans* was investigated (*14*). The biomass demonstrated to possess a superb performance in biosorption of uranium under acidic conditions (pH 2.5–4.0) where the maximum uranium binding exceeded 2.0 mmol/g biomass. During the 1-month continuous-flow column operation with multiple biosorption–desorption cycles, *Sargassum* biomass was stable with a high uranium uptake of 105 mg/g before the breakthrough occurred. This demonstrated its encouraging potential for biosorption technology industrial applications. Equilibrium sorption isotherm principles are usually used to quantitatively evaluate the heavy metal uptake performance of different biosorbents. Langmuir and Freundlich models often generally fit the isotherm relationships. The Langmuir model is based on the monolayer sorption mechanism, and its two parameters reflect the maximum metal uptake and the metal affinity toward the sorbent. Freundlich model parameters are more empirical. While it has been revealed that protons play a crucial role in biosorption, especially for marine algae biomass, the effect of protons is not taken into account in mathematical sorption models, including the classical ones by Langmuir and Freundlich. The usual practice is to determine a series of separate isotherm models for different pH values.

Since the biosorption of uranium is largely an ion exchange process (*15*, *16*), the use of the ion exchange constants is more appropriate. However, the complex composition of biomass materials makes it more difficult to handle their behavior theoretically as compared to well-defined simple synthetic ion-exchange resins. The difficulty of determining the activity coefficient in the biomass material results in very tedious calculation procedures involved in attempts to predict the equilibrium metal uptakes when the ion exchange constant approach is used. Schiewer and Volesky (*17*) proposed an ion-exchange isotherm equation for biosorption of cadmium, copper and zinc. The proton concentration was incorporated into the equation as an independent variable so that the prediction of biosorption metal uptake at various solution pH values became an easy explicit calculation. The limitation of this model is in that it did not take into consideration the effect of metal ion hydrolysis in aqueous solutions on biosorption performance. Guibal et al. (*7*) observed the dependency of uranium hydrolysis on the solution pH. Earlier work (*18*) established unusually high uranium uptakes at pH 3.5–4.0; more uranium sequestered than would correspond to the stoichiometric number of biomass binding sites. This was attributed to the particular speciation of uranium ions in the aqueous solution. Mathematical models reflecting this phenomenon are rare in the literature.

This work combines the hydrolysis of uranium ions in the aqueous solution with uranium-proton biosorption ion exchange. Based on this broader concept, a new mathematical model is proposed to describe the uranium equilibrium binding to the preprotonated seaweed biomass at a wide range of equilibrium uranium solution concentrations or biomass loadings. The solution pH is incorporated into the model equation as an independent variable.

Materials and Methods

Sorbent Preparation. A batch of beach-dried brown seaweed *Sargassum fluitans* biomass, collected in Naples, FL, was contacted with 0.1 N HCl (10 g biomass/L) for 3 h to standardize the biomass by eliminating the light metals Ca^{2+}, Mg^{2+}, etc. originally trapped in the seaweed. The biomass was then rinsed with deionized water in the same volume 5–7 times until a stable wash solution pH 4.0 was reached. During each rinse, the biomass was soaked for about 15 min. Biomass drying in an oven at 40–60 °C overnight followed. The natural shape and leafy structure of the seaweed plant were not destroyed during the acid protonation treatment, and the material was stored for later use.

Metal Concentration Analysis. Dissolved uranium concentrations in solution were determined by an inductively coupled plasma atomic emission spectrophotometer (ICP-AES, Thermo Jarrel Ash, Model TraceScan). The ICP analyses

* Corresponding author phone: (514)398-4276; fax: (514)398-6678; e-mail: boya@chemeng.lan.mcgill.ca.

were conducted at wavelengths of 409.014 nm. At this wavelength, the linear concentration range is up to 20.0 mgU/L.

Sorption Equilibrium Experiments. A sorption dynamics methodology was used to establish that 3–4 h of contact was an adequate time to attain the sorption equilibrium. The details of sorption dynamics were described earlier (*14*). With parallel control samples containing no biomass, a series of 50 mL of uranium nitrate solution concentrations, ranging 10–2000 ppm, were mixed with 0.1 g of biomass in 150 mL Erlenmeyer flasks. The flasks were agitated on a rotary shaker at 3 Hz at room temperature. The solution pH was adjusted to the desired values with 0.1 N LiOH or 0.1 N HCl. When the sorption equilibrium was reached 3 h after the solution pH stabilized at the desired value, the suspension was filtered or centrifuged. The filtration was conducted with 0.5 μ Millipore membranes. The centrifuge was operated at 5000 rpm for 20 min. The supernatant was diluted with D–H$_2$O to reach the linear concentration calibration range as required for the metal concentration analysis by the ICP-AES. The recovered biomass was soaked in deionized water for about 15 min. Wash water was decanted and the wash repeated two more times. The preliminary experiments showed that neither sorption of dissolved metals occurred on the filter assembly or plastic centrifuge tubes nor biosorbed metal loss occurred during the soaking. The biomass was dried at 40–60 °C in an oven overnight. The dried metal-loaded biomass was used in desorption experiments later.

The uranium uptake was calculated from the concentration difference method that is based on the mass balance as follows

$$q_U = (U_i - U_f) \, V/W \qquad (1)$$

with V being the solution volume and W being the mass of biosorbent. The initial uranium concentration U_i corresponds to the control samples, and the final uranium concentration U_f was determined for the supernatant solution after the sorption contact.

Acid Elution. In the desorption experiments, 0.1 g of dry metal-loaded biomass was mixed with 50 mL of 0.1 N HCl in a 150 mL Erlenmeyer flask. After 3–4 h, the uranium concentration in the desorbing solution was determined using the same procedure as for the sorption equilibrium experiments. No pH adjustment was required because the change of proton concentration caused by the elution of uranium metal ions was negligible compared with the elutant acidity. The amount of uranium metal desorbed from the biomass could be calculated as follows

$$q_{des} = C_{des} V/W \qquad (2)$$

where q_{des} is the eluted metal content per gram of biomass and C_{des} is the metal concentration in the HCl desorbing solution.

Mathematical Model

Model Assumptions. It would be helpful and time-saving to have a mathematical model capable of predicting the final uranium metal uptake from given initial conditions. The metal ion binding in biosorption could be attributed to several mechanisms such as ion exchange, complexation, electrostatic attraction, and microprecipitation (*19*). For algal biomass, ion exchange was shown to play an important role in the metal sequestering mechanism (*20–22*). In more details, the following assumptions were made for the hydrolyzed ion exchange model (HIEM).

1. In the range of acidic to near neutral pH values, the uranium cation UO_2^{2+} is hydrolyzed in an aqueous solution. The fo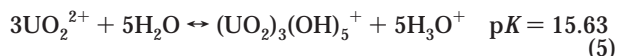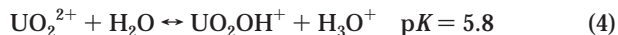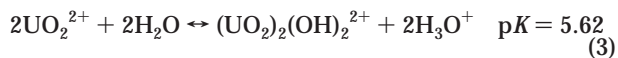ur major hydrolyzed complex ions, UO_2^{2+}, $(UO_2)_2$-$(OH)_2^{2+}$, UO_2OH^+, and $(UO_2)_3(OH)_5^+$, exist in a hydrolysis equilibrium in the aqueous solution. The repartitioning of hydrolyzed uranium species depends on the solution pH and on the total uranium concentration in the solution.

2. The ion exchange reaction is taking place between various hydrolyzed uranium ions and protons in the biomass binding sites, and an equilibrium will be reached for all forms of complex uranium ions.

3. The total uranium uptake consists of the binding of all forms of hydrolyzed uranium ions by biomass.

4. All types of possible biomass binding sites have the same affinity to uranium cations.

Model Development. The hydrolysis equilibrium of uranium metal ions are as follows (*23*)

$$2UO_2^{2+} + 2H_2O \leftrightarrow (UO_2)_2(OH)_2^{2+} + 2H_3O^+ \quad pK = 5.62 \qquad (3)$$

$$UO_2^{2+} + H_2O \leftrightarrow UO_2OH^+ + H_3O^+ \quad pK = 5.8 \qquad (4)$$

$$3UO_2^{2+} + 5H_2O \leftrightarrow (UO_2)_3(OH)_5^+ + 5H_3O^+ \quad pK = 15.63 \qquad (5)$$

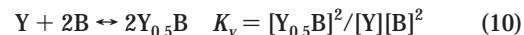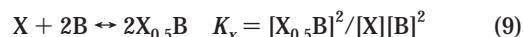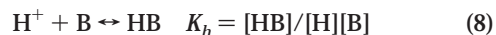where pKs are the negative logarithms of the equilibrium constants.

As indicated by the high pK value of eq 5, the amount of hydrolyzed ion $(UO_2)_3(OH)_5^+$ in the aqueous uranium solution system should be rather low. Thus its effect on the biosorption of uranium could be neglected. The hydrolysis equilibrium constants for eq 3 and 4 are expressed in the following manner

$$K_{ey} = \frac{[Y][H]^2}{[X]^2} \qquad (6)$$

$$K_{ez} = \frac{[Z][H]}{[X]} \qquad (7)$$

where K_{ey} and K_{ez} are the equilibrium constants for eqs 3 and 4, respectively. X, Y, and Z represent ionic species UO_2^{2+}, $(UO_2)_2(OH)_2^{2+}$, and $(UO_2)(OH)^+$, respectively.

Based on the assumption of ion exchange between the hydrolyzed uranium ions and protons on the biomass binding sites, the following equilibrium equations are proposed

$$H^+ + B \leftrightarrow HB \quad K_h = [HB]/[H][B] \qquad (8)$$

$$X + 2B \leftrightarrow 2X_{0.5}B \quad K_x = [X_{0.5}B]^2/[X][B]^2 \qquad (9)$$

$$Y + 2B \leftrightarrow 2Y_{0.5}B \quad K_y = [Y_{0.5}B]^2/[Y][B]^2 \qquad (10)$$

$$Z + B \leftrightarrow ZB \quad K_z = [ZB]/[Z][B] \qquad (11)$$

where K_h, K_x, K_y, and K_z are equilibrium formation constants corresponding to the bound components formed between various hydrolyzed uranium ions and protons with biomass in the solution. The formulation for the complex divalent uranium ionic group and biomass binding site is chosen as $2M_{0.5}B$ instead of MB_2. This is to emphasize that not only the electrostatic attraction but also all the complexation are relevant in this case where two bonds between the metal ion and biomass have to be broken in competitive binding or in desorption of the metal from biomass (*22, 24*).

The total binding sites on the biomass are distributed among all the bound forms of hydrolyzed uranium ions and protons as well as the residual free sites

$$C_t = [B] + [HB] + [X_{0.5}B] + [Y_{0.5}B] + [ZB] \qquad (12)$$

where C_t and [B] are the concentrations of the total and free binding sites, respectively.

Upon substituting eqs 6–11 into eq 12, the concentration of free binding sites in the equilibrium system is obtained

as follows:

$$[B] = \cfrac{C_t}{1 + K_h[H] + K_x[X] + \cfrac{[X]}{[H]}(\sqrt{K_{ey}K_y} + K_{ez}K_z)} \qquad (13)$$

Substituting eq 13 into eqs 8−11, respectively, we obtain

$$q_H = [HB] = \cfrac{C_t K_h[H]}{1 + K_h[H] + K_x[X] + \cfrac{[X]}{[H]}(\sqrt{K_{ey}K_y} + K_{ez}K_z)} \qquad (14)$$

$$[X_{0.5}B] = \cfrac{C_t\sqrt{K_x[X]}}{1 + K_h[H] + K_x[X] + \cfrac{[X]}{[H]}(\sqrt{K_{ey}K_y} + K_{ez}K_z)} \qquad (15)$$

$$[Y_{0.5}B] = \cfrac{C_t\cfrac{[X]}{[H]}\sqrt{K_{ey}K_y}}{1 + K_h[H] + K_x[X] + \cfrac{[X]}{[H]}(\sqrt{K_{ey}K_y} + K_{ez}K_z)} \qquad (16)$$

$$[ZB] = \cfrac{C_t\cfrac{[X]}{[H]}K_{ez}K_z}{1 + K_h[H] + K_x[X] + \cfrac{[X]}{[H]}(\sqrt{K_{ey}K_y} + K_{ez}K_z)} \qquad (17)$$

Equation 14 could be used for the calculation of proton sorption on the biomass at any given uranium concentration level and solution pH. The total uranium uptake q_U is assessed as the sum of all the bound forms of hydrolyzed uranium ions, i.e.:

$$q_U = 0.5[X_{0.5}B] + (2 \times 0.5)\,[Y_{0.5}B] + [ZB] \qquad (18)$$

Upon substitution of $[X_{0.5}B]$, $[Y_{0.5}B]$, and $[ZB]$ from eqs 15−17 we obtain:

$$q_U = \cfrac{C_t\!\left(0.5\sqrt{K_x[X]} + \cfrac{[X]}{[H]}(\sqrt{K_{ey}K_y} + K_{ez}K_z)\right)}{1 + K_h[H] + K_x[X] + \cfrac{[X]}{[H]}(\sqrt{K_{ey}K_y} + K_{ez}K_z)} \qquad (19)$$

In eq 19, the uranium uptake could be calculated from the solution pH or proton concentration [H] and the concentration of the free uranium ion UO_2^{2+}, [X]. Although the mathematical form of eq 19 is similar to that for the multicomponent Langmuir sorption isotherm as adapted from Hill (25), the mechanism that lies behind is completely different. The present model considers ion exchange, not only a simple competition for free binding sites where no reverse reaction takes place. In eq 19, the concentration of the free uranium ion [X] is not necessarily the same as the total uranium concentration in the solution because of the hydrolysis of the uranium ion in the solution. Only the total uranium concentration was measurable experimentally and [X] must be quantified from it using hydrolysis equilibrium calculations. Usually, this could be done by using the computer program MINEQL+ (19) as done by Guibal et al. (7) and by Yang and Volesky (14). However, it would be more useful to derive a formula expressing the concentration of the complex ions as an explicit function of the measurable total uranium concentration and the pH value.
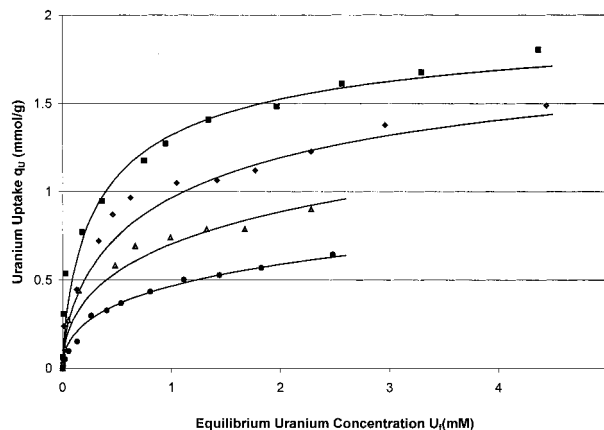

FIGURE 1. Influence of solution pH on uranium sorption isotherms: Comparison of experimental data and HIEM regression. Experimental data: (●) pH 2.5; (▲) pH 3.0; (◆) pH 3.5; (■) pH 4.0; and (—) HIEM model regressed value.

The total uranium concentration U_f in the solution consists of free ions and all major hydrolyzed ions:

$$U_f = [UO_2^{2+}] + 2[(UO_2)_2(OH)_2^{2+}] + [(UO_2)(OH)^+]$$

$$= [X] + 2[Y] + [Z] \qquad (20)$$

Substituting eqs 6 and 7 into 20, the concentration of free ions UO_2^{2+} in the solution was obtained as the following correlation:

$$[X] = \cfrac{[H](\sqrt{([H] + K_{ez})^2 + 8K_{ey}U_t} - ([H] + K_{ez}))}{4K_{ey}} \qquad (21)$$

Finally, eqs 14, 19, and 21 express the proton uptake and the uranium biosorption uptake as an explicit function of the total uranium concentration and the solution pH value, which fulfills the main modeling objective.

Determination of Model Parameters. The other parameters required for the calculation include K_{ey} and K_{ez}, the hydrolysis equilibrium constants for uranium ions UO_2^{2+} which could be calculated from the values of pKs in eqs 3 and 4. The four biosorption equilibrium constants, K_h, K_x, K_y, and K_z for protons and complex hydrolyzed uranium ions UO_2^{2+}, $(UO_2)_2(OH)_2^{2+}$, and UO_2OH^+ should be regressed from the uranium sorption isotherm experimental data at various pH levels. The total binding capacity of biomass, C_t, could be determined by acid−base titration of the protonated biomass.

The nonlinear least-squares method was used to find the optimal combination of the parameter sets. The objective function for the optimal regression was as follows where φ

$$\varphi = \sum_i^N (q_{model} - q)_{exp\,i}^2 \qquad (22)$$

is the least-squares error, i is the experimental sample number, and N is the number of samples. While q_{exp} represents the experimental uranium biosorption uptake, q_{model} stands for that calculated from model eqs 19 and 21. A computer program in MATLAB (26) was developed for the regression procedure.

Results and Discussion

Uranium Sorption Isotherms at Different pH. Experimental isotherm points for equilibrium uranium biosorption on *Sargassum* biomass at pH 2.5, pH 3.0, pH 3.5, and pH 4.0 are plotted in Figure 1. Each of these isotherms could be

TABLE 1. Parameters for Langmuir Model

	pH 2.5	pH 3.0	pH 3.5	pH 4.0
K (mmol/L)	0.4839	0.1529	0.1087	0.1127
q_m (mmol/g)	0.7275	0.8720	1.2652	1.5856
R^a	0.996	0.993	0.976	0.960

^{a} R is the correlation coefficient.

TABLE 2. Parameters for HIEM Model^a

C_t (mmol/g)	K_h (L/mol)	K_x (L/mol)	K_y (L/mol)	K_z (L/mol)
2.25	235.1	1081.7	1.7731×10^4	1.1494×10^4

^{a} The correlation coefficient is 0.99.
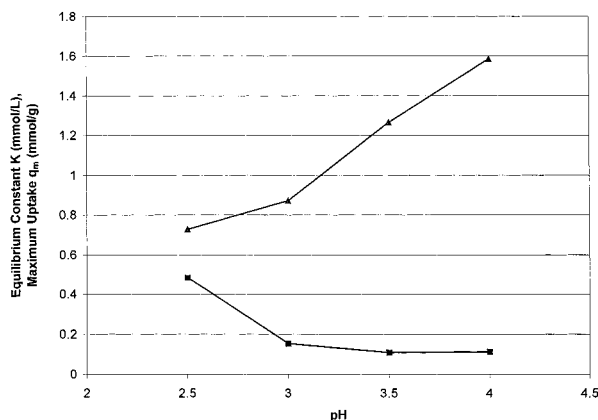
FIGURE 2. Influence of the solution pH on Langmuir sorption isotherm model parameters: (▲) maximum uranium uptake q_m (mmol/g) and (■) sorption equilibrium constant K (mmol/L).
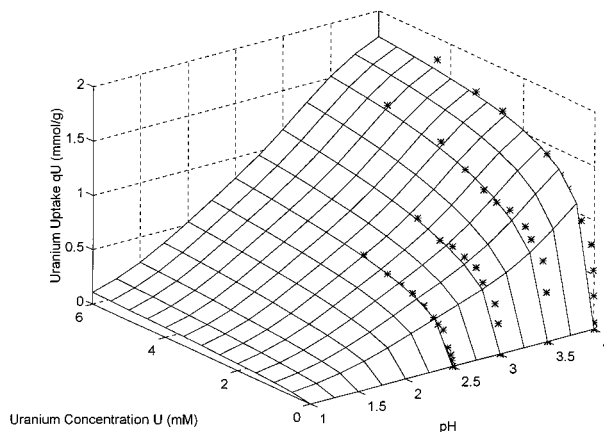

FIGURE 3. Uranium sorption isotherm experimental data and HIEM model regression at solution pH 2.5−4.0 and uranium metal concentration 0.0−6.0 mmol/L. (∗) experimental and (mesh) HIEM model.
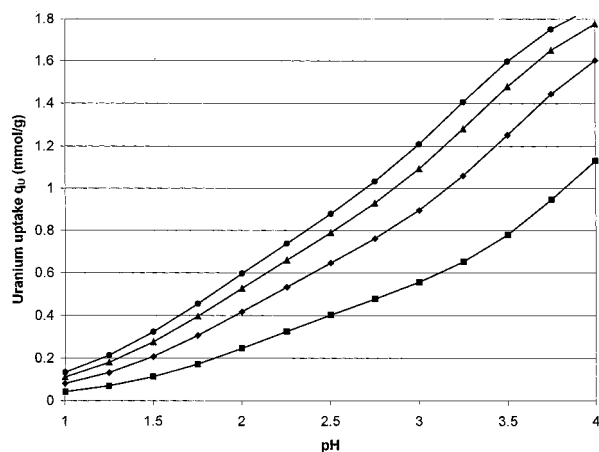

FIGURE 4. Influence of the solution pH on the uranium sorption uptake at constant uranium equilibrium concentrations: (●) $U_f =$ 6.0 (mmol/g), (▲) $U_f = 4.0$ (mmol/g), (◆) $U_f = 2.0$ (mmol/g), and (■) $U_f = 0.5$ (mmol/g).

represented by a Langmuir model. The Langmuir model parameters were obtained with an nonlinear regression using KaleidaGraph software as listed in Table 1. q_m is the maximum uptake capacities, and K is the equilibrium constant in the Langmuir model. The Langmuir model parameters were largely dependent on the solution pH values at sorption equilibrium, as plotted in Figure 2. The maximum sorption capacity q_m increased while the Langmuir equilibrium constant K decreased for higher solution pH values, indicating that the sorption affinity of uranium for the biomass was enhanced at higher solution pH values. It is also worth noting that the q_m values in equivalence units at pH 3.5 and pH 4.0 were 2.53 and 3.17 meq/g, respectively, which exceeded the maximum amount of the biomass binding sites, 2.25 meq/g. The control samples demonstrated that the very high uranium uptake could not be attributed to microprecipitation. This phenomenon could not be explained by the ion exchange between UO_2^{2+} and protons either. The hydrolyzed ion exchange model (HIEM) could cover this case very well.

HIEM Model. The first model parameter C_t, the amount of the biomass binding sites, was determined as 2.25 mmol/g by acid−base titration of the *Sargassum* biomass (*27, 28*). At pH 2.5, 99.7% of total uranium exists in the form of the free ion UO_2^{2+} in the aqueous solution according to the calculation results from the computer program MINEQL+ (*19*) in the concentration range of 0−10 mM. Thus the effect of the hydrolyzed ions $(UO_2)_2(OH)_2^{2+}$ and UO_2OH^+ was not significant in this situation. Thus, setting the values of K_y and K_z to zero shall be a good initial guess. K_h and K_x were regressed then from the curve-fitting of experimental biosorption data at pH 2.5. Next, K_y and K_z were determined by using experimental data at other pH values. The procedure was repeated by substituting the regressed values of K_y and K_z for curve-fitting at pH 2.5 until a stable set of parameters were obtained, as listed in Table 2. Using the obtained model parameters, the model equations could be applied to predict uranium biosorption isotherms at any given pH values, for instance, at pH 3.5 and pH 4.0. The regressed model curves at pH 2.5 and pH 3.0 and the model-predicted curves at pH 3.5 and pH 4.0 are demonstrated with the corresponding experimental points in Figure 1. The correlation coefficient

of the regression is 0.99, and the model-predicted values match the isotherm experimental points at pH 3.5 and pH 4.0 within an average of 5% deviation.

The model-calculated uranium uptake is plotted as a 3-D surface against two independent variables, pH and the equilibrium uranium concentration, in Figure 3. The scattered points represent the experimental uranium uptakes that are higher than the corresponding model calculated values. Those values that are lower than the model-calculated ones are hidden by the model surface. With the increase in pH and uranium concentration, the elevation of the plotted uptake surface increases. To demonstrate the effect of pH on the uptake, a series of surface cut curves at given uranium equilibrium concentrations was plotted in Figure 4. Although the effect of the pH on the uptake is somewhat more pronounced at higher uranium concentrations, the uptake increase with the pH is flat for all uranium concentrations chosen in the graph.

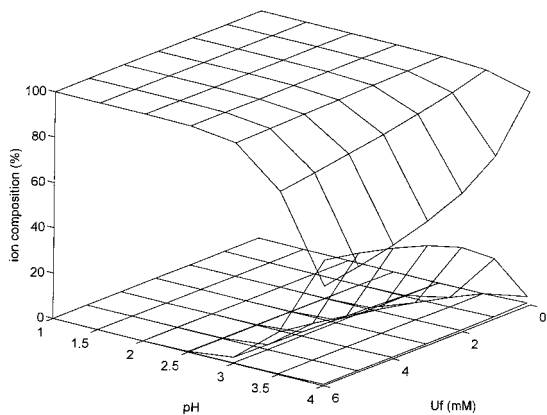**Uranium Ionic Distribution in Solution and Biomass.** The distribution of hydrolyzed uranium ions in the aqueous

FIGURE 5. Distribution of the hydrolyzed ionic uranium species in the solution: (top mesh) UO_2^{2+}, (middle mesh) $(UO_2^{2+})_2(OH)_2^{2+}$, and (bottom mesh) $(UO_2^{2+})(OH)^+$.
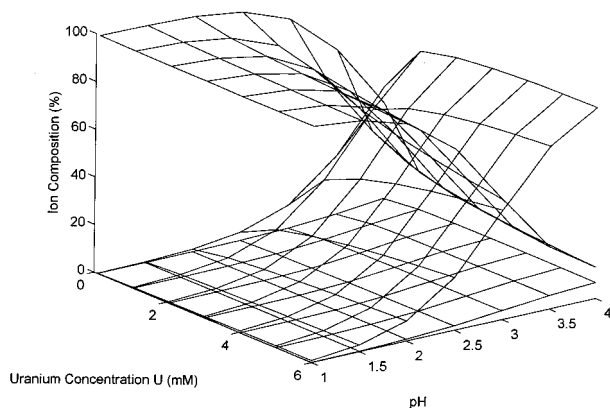

FIGURE 6. Distribution of the hydrolyzed ionic uranium species in the biomass: (top mesh) UO_2^{2+}, (middle mesh) $(UO_2^{2+})_2(OH)_2^{2+}$, and (bottom mesh) $(UO_2^{2+})(OH)^+$.

solution is dependent on both the solution pH and total uranium concentration. This could be quantified from the hydrolysis equilibrium by using the model eqs 6, 7, and 21. The calculated results are demonstrated in Figure 5 where the *x*-axis represents the solution pH value, the *y*-axis is for the uranium normality in solution, and the surfaces represent percentages of various uranium ionic species. When the solution pH values were below pH 2.7, the UO^{2+} was the predominant species. Above pH 2.7, the percentage of UO_2^{2+} started to decrease with the solution pH, while that of $(UO_2)_2$-$(OH)_2^{2+}$ increased with the pH and total uranium concentration. At pH 4.0 and 6 mM uranium equilibrium concentration, more than 50% of uranium ions existed in the form of divalent $(UO_2)_2(OH)_2^{2+}$. The monovalent UO_2OH^+ was lower than 1% even at higher pH and uranium concentrations.

Compared with the uranium distribution in solution, biomass attracted a higher proportion of uranium complex ions as demonstrated in Figure 6. The ionic distribution in the solid biomass phase was calculated by using eqs 15−17. $(UO_2)_2(OH)_2^{2+}$ ions already existed even at very low pH values. For instance, there was more than 20% of bound uranium in the form of $(UO_2)_2(OH)_2^{2+}$ at pH 2.5. In addition, although in a relatively lower percentage, UO_2OH^+ ion existed at a wide range of pH values. This indicated that the complex ion species may have relatively high affinity to the biomass binding sites. Figures 7 and 8 visualize the contribution of the free uranium ion UO_2^{2+} and the hydrolyzed ion $(UO_2)_2(OH)_2^{2+}$ to the total uranium uptake by the biomass, respectively. At a low pH 2.5, the bound uranium consisted predominantly of UO_2^{2+} ions, while the uranium uptake at pH 4.0 was mainly contributed by the binding of $(UO_2)_2(OH)_2^{2+}$.
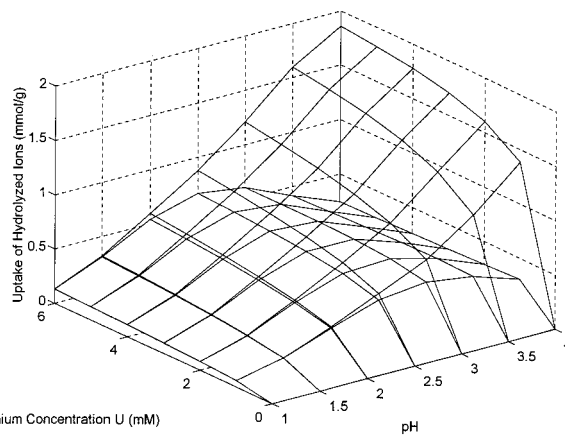

FIGURE 7. Influence of the solution pH and the equilibrium total uranium concentration on the contribution of UO_2^{2+} ionic species to the total uranium uptake: (top mesh) total uranium uptake (mmol/g) and (lower mesh) uptake of UO_2^{2+} (mmol/g).
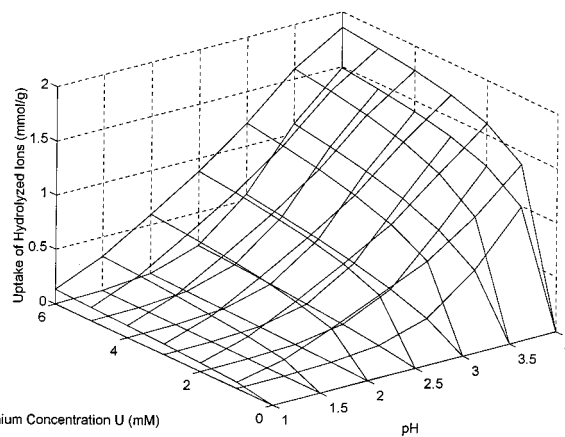

FIGURE 8. Influence of the solution pH and the equilibrium total uranium concentration on the contribution of $(UO_2^{2+})_2(OH)_2^{2+}$ ionic species to the total uranium uptake: (top mesh) total uranium uptake (mmol/g) and (lower mesh) uptake of $(UO_2^{2+})_2(OH)_2^{2+}$ (mmol/g).

For each hydrolyzed ion $(UO_2)_2(OH)_2^{2+}$ bound, two binding sites would be occupied. However, since there are two uranium atoms in this complex ion, the equivalence of the uranium atom itself was accounted as one in this case instead of two as for UO_2^{2+} binding. In other words, the hydrolyzed ion $(UO_2)_2(OH)_2^{2+}$ behaves like a monovalent ion in biosorption and thus enhances the overall uranium uptake significantly. While this phenomenon was qualitatively discussed in our earlier work (*18*), the results of quantitative model calculations are now demonstrated in Figure 8.

Prediction of the Equilibrium Uranium Concentration in Acid Elution. If the initial uranium concentration in the biosorbent (or the initial uranium loading for elution) and the solution pH were specified, the final equilibrium uranium concentration and uptake could be obtained by iterating eqs 19 and 21 with the sorption mass balance in eqs 1 or 2. In Figure 3, the altitude of the uranium uptake surface decreases rapidly when the solution pH decreases. This indicates that the metal-laden biomass could be efficiently eluted under acidic conditions. HCl (0.1 N) was capable of removing cadmium, copper, and zinc from the *Sargassum* seaweed biomass well (*29*). The desorption of uranium from the *Sargassum* seaweed biomass with 0.1 N HCl is also complete without damaging the biomass structures (*18*). Figure 9 demonstrates the prediction result of eluting uranium-laden biomass with 0.1 N HCl, using the biomass/acid (S/L) ratio of 2.0 g/L. The *x*-axis represents the initial uranium loading and the *y*-axis is for the uranium concentration in the acid
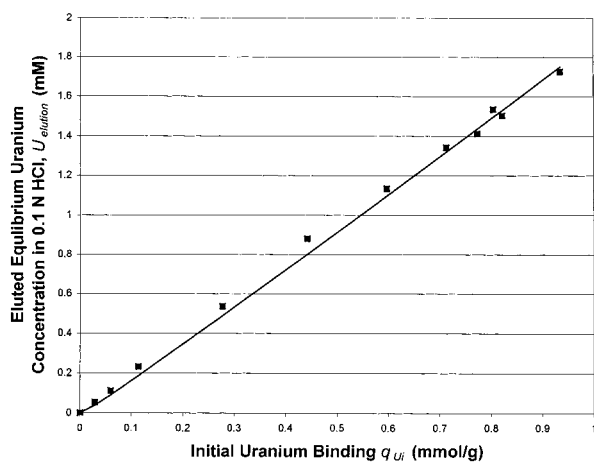
FIGURE 9. HIEM model prediction of the uranium eluting concentration in 0.1 N HCl: (■) experimental and (—) model predicting line, slope = 2.06.

elutant. The slope of the model curve is 2.06, which indicated that the uranium mass balance closes well. The model-calculated curve and the experimental points agreed well, and the average deviation was less than 5%.

Finally, it must be indicated that the heterogeneity and chemical fabric of biomass may affect the accuracy of the model prediction. In the *Sargassum fluitans* biomass, the carboxyl and sulfate groups were identified as active binding sites (*28*, *30*), and carboxyl groups, mainly of alginate, are considered to play a major role in the biosorption of heavy metals (*30*). Although model assumption 4 whereby all binding sites in the biomass have the same affinity for the uranium cations would not cause a significant error, a multiple-site model would be more adequate to address this issue at a price of increasing complexity.

The mathematical model based on the ion exchange between hydrolyzed uranium ions and protons originally on the biomass incorporated the proton concentration into model equations in addition to the total uranium concentration and the hydrolysis equilibrium constants. The model could predict the equilibrium status from the initial conditions for both uranium biosorption and acid desorption. The influence of the pH values on uranium biosorption under acidic conditions was well described by the model-calculated curves which agreed with the experimental biosorption isotherm and acid elution data within an average deviation of 5%.

The hydrolysis of uranium ions plays an important role in biosorption by protonated *Sargassum fluitans* seaweed. The hydrolyzed uranium ions, especially the divalent $(UO_2)_2(OH)_2^{2+}$ made a significant contribution to the total biosorption uranium uptake which is very high and quite encouraging for this biosorption process application considerations.

Glossary

[ ]	representative of concentration for the bracketed species (mmol/L)
B	representative of free biomass binding sites
C_i, C_f	initial or final uranium metal concentration (mmol/L)
C_{des}	uranium metal concentration in the eluting solution (mmol/L)
C_t	total concentration of binding sites on the biomass (mmol/g)
H	representative of proton (mmol/L)
i	index number of the experimental points in eq 22
K	Langmuir equilibrium constant (mmol/L)
K_h	equilibrium formation constant of proton and biomass in eq 8 (L/mol)
K_x	equilibrium formation constant of UO_2^{2+} and biomass in eq 9 (L/mol)
K_y	equilibrium formation constant of $(UO_2)_2(OH)_2^{2+}$ and biomass in eq 10 (L/mol)
K_z	equilibrium formation constant of $(UO_2)(OH)^+$ and biomass in eq 11 (L/mol)
K_{ey}	hydrolysis equilibrium constant for eq 3
K_{ez}	hydrolysis equilibrium constant for eq 4
N	total number of experimental points in eq 22
q_{des}	eluted metal content per gram of biomass (mmol/g)
q_{exp}	experimental value of metal uptake (mmol/g)
q_H	uptake of proton on biomass (mmol/g)
q_m	Langmuir maximum uptake (mmol/g)
q_{model}	model-calculated value of metal uptake (mmol/g)
q_U	uptake of uranium on biomass (mmol/g)
S_t	total surface area of biomass particles (cm²)
V	solution volume (L)
W	biomass weight (g)
X	representative of UO_2^{2+} (mmol/L)
Y	representative of $(UO_2)_2(OH)_2^{2+}$ (mmol/L)
Z	representative of $(UO_2)(OH)^+$ (mmol/L)
φ	objective function for curve fitting in eq 22

Literature Cited

(1) Ashley, N. V.; Roach, D. J. W. *J. Chem. Technol. Biotechnol.* **1990**, *49*, 381−394.
(2) Macaskie, L. E. *CRC Crit. Rev. Biotechnol.* **1991**, *11*, 41−112.
(3) Benedict, B.; Pigford, T. H.; Levi, H. W. *Nuclear Chemical Engineering*; McGraw-Hill: New York, 1981.
(4) White, S. K. *J. Am. Water Works Assoc.* **1983**, *75*, 374.
(5) Laul, J. C. *Radioanal. Nucl. Chem. Articles* **1992**, *156*, 235.
(6) Volesky, B.; Tsezos, M. **1981**. U.S. Patent 4320 093; Canadian Patent 1143 007 (1983).
(7) Guibal, E.; Roulph, C.; Le Cloirec, P. *Water Res.* **1992**, *26*, 1139−45.
(8) Macaskie, L. E.; Empson, R. M.; Cheetham, A. K.; Grey, C. P.; Skarnulis, A. J. *Science* **1992**, *257*, 782−784.
(9) Munroe, N. D. H.; Bonner, J. D.; Williams, R.; Pattison, K. F.; Norman, J. M.; Faison, B. D. In *Abstracts, American Society for Microbiology Annual Meeting*; American Society of Microbiology: Washington, DC, 1993.
(10) Hu, M. Z.-C.; Norman, J. M.; Faison, N. B.; Reeves, M. *Biotechnol. Bioeng.* **1996**, *51*, 237−247.
(11) Horikoshi, T.; Nakajima, A.; Sakaguchi, T. *Agric. Biol. Chem.* **1979**, *332*, 617.
(12) Byerley, J. J.; Scharer, J. M.; Charles, A. M. *Chem. Eng. J.* **1987**, *36*, B49−B59.

(13) Edgington, D. N.; Gorden, S. A.; Thommes, M. M.; Almodovar, L. R. *Limnol. Ocean.* **1970**, *15*, 945−955.

(14) Yang, J.; Volesky, B. In *Biohydrometallurgy and the Environment Toward the Mining of the 21st Century (Part B): International Biohydrometallurgy Symposium − Proceedings*; Amils, R., Ballester, A., Eds.; Elsevier: Amsterdam, The Netherlands, 1999; Vol. B, pp 483−492.

(15) Crist, R. H.; Martin, J. R.; Guptill, P. W.; Eslinger, J. M.; Crist, D. R. *Environ. Sci. Technol.* **1990**, *24*, 337−342.

(16) Kuyucak, N.; Volesky, B. *Biotechnol. Bioeng.* **1989**, *33*, 809−814.

(17) Schiewer, S.; Volesky, B. *Environ. Sci. Technol.* **1996**, *30*, 2921−2927.

(18) Yang, J.; Volesky, B. *Water Res.* **1999**, in press.

(19) Westall, J. C.; Zachary, J. L.; Morel, F. M. M. In *Oregon State University Report No. 86-01 Version 1*; Oregon State University: Eugene, OR, 1986.

(20) Crist, R. H.; Oberholser, K.; Schwartz, D.; Marzoff, J.; Ryder, D.; Crist, D. R. *Environ. Sci. Technol.* **1988**, *22*, 755−760.

(21) Crist, D. R.; Crist, R. H.; Martin, J. R.; Watson, J. In *Metals-Microorganisms Relationships and Applications, FEMS Symposium Abstracts, Metz, France, May 5−7*; Bauda, P., Ed.; Societe Francaise de Microbiologie: Paris, France, 1993; p 13.

(22) Schiewer, S.; Volesky, B. *Environ. Sci. Technol.* **1995**, *29*, 3049−3058.

(23) Baes, C. F. J.; Mesmer, R. E. *The Hydrolysis of Cations*; Wiley-Interscience: John Wiley & Sons: New York, 1976; pp 197−240.

(24) Buffle, J. *Complexation Reactions in Aquatic Systems: An Analytical Approach*; Ellis Horwood Ltd.: Chichester, U.K., 1988; pp 156−157, 280−283, 323.

(25) Hill, C. G. J. *An Introduction to Chemical Engineering Kinetics and Reactor Design*; John Wiley & Sons: New York, 1977; pp 167−204.

(26) Mathworks, I. *MATLAB Version 4.0 for Microsoft Windows*; MathWorks, Inc.: Natick, MA, 1993.

(27) Schiewer, S.; Fourest, E.; Chong, K. H.; Volesky, B. In *Biohydrometallurgical Processing: Proceedings of the International Biohydrometallurgy Symposium*; Jerez, C. A., Vargas, T., Toledo, H., Wiertz, J. V., Eds.; University of Chile: Santiago, 1995; Vol. 2, pp 219−228.

(28) Fourest, E.; Volesky, B. *Environ. Sci. Technol.* **1996**, *30*, 277−282.

(29) Aldor, I.; Fourest, E.; Volesky, B. *Can. J. Chem. Eng.* **1995**, *73*, 516−522.

(30) Fourest, E.; Volesky, B. *Appl. Biochem. Biotechnol.* **1997**, *67*, 33−44.